Molecular Crystals and Liquid Crystals

ISSN: 1542-1406 (Print) 1563-5287 (Online) Journal homepage: https://www.tandfonline.com/loi/gmcl20

Investigation of Address Discharge and Efficiency Characteristics by Thickness of Phosphor Layer in Microplasma Cells

Hyung Dal Park , Jae Hyun Kim , Heung-Sik Tae & Bo-Sung Kim

To cite this article: Hyung Dal Park , Jae Hyun Kim , Heung-Sik Tae & Bo-Sung Kim (2012) Investigation of Address Discharge and Efficiency Characteristics by Thickness of Phosphor Layer in Microplasma Cells, Molecular Crystals and Liquid Crystals, 564:1, 104-111, DOI: 10.1080/15421406.2012.691697

To link to this article: https://doi.org/10.1080/15421406.2012.691697

Published online: 20 Aug 2012.

Mol. Cryst. Liq. Cryst., Vol. 564: pp. 104–111, 2012

ISSN: 1542-1406 print/1563-5287 online
DOI: 10.1080/15421406.2012.691697

Taylor & Francis
Taylor & Francis Group

Investigation of Address Discharge and Efficiency Characteristics by Thickness of Phosphor Layer in Microplasma Cells

HYUNG DAL PARK,[1] JAE HYUN KIM,[2] HEUNG-SIK TAE,[2,*] AND BO-SUNG KIM[3]

[1]Radiation Instrumentation Research Division, Korea Atomic Energy Research Institute, Daejeon 305-353, Korea
[2]School of Electrical Engineering, College of IT Engineering, Kyungpook National University, Daegu 702-701, Korea
[3]Display Nanomaterials Institute, Kyungpook National University, Daegu 702-701, Korea

This paper analyzes the address discharge characteristics in the red, green, and blue cells, respectively by using the Vt closed-curve analysis method. To reduce the difference of the address discharge delay among the R, G, and B cells, the effects of the phosphor thickness on the address discharge delay are examined. By controlling properly the phosphor thickness among the R, G, and B cells, the difference of the address discharge delay is observed to be minimized among the R, G, and B cells. In addition, the luminous efficacy was observed to be improving by increase the phosphor layer thickness.

Keywords Luminous efficacy; photoluminescence; phosphor layer thickness; address discharge characteristics; Vt closed-curve

Introduction

The stable address discharge is still essential for the low cost high image quality ac-plasma display panel. In particular, the stable address discharge delay characteristics irrespective of the R, G, and B cell difference is the most important factor for the realization of the high-speed address under wider dynamic driving margin in the plasma display panel with millions of micro-discharge cells [1–6]. However, the firing voltages of the plate gap discharge are different mainly due to the R, G, and B cells, thus resulting in the unstable address discharge. Moreover, the problems related to low luminance efficacy continue to be issues in plasma display panel. The phosphor layer thickness may also be factor that affects the luminance and luminous efficiency of the plasma display panel [7–9].

Accordingly, this paper investigates that the discharge characteristics of the R, G, and B cells are analyzed and compared by using the Vt closed-curve analysis. To reduce the address discharge delay time difference among the R, G, and B cells, the address discharge characteristics are analyzed by varying the phosphor thicknesses of the R, G,

*Address correspondence to Prof. Heung-Sik Tae, Kyungpook National University, Sangyuk-dong, Buk-gu, Daegu 702-701, Korea (KOR). Tel: (+82)53-950-6563; Fax: (+82)53-950-5505. E-mail: hstae@ee.knu.ac.kr

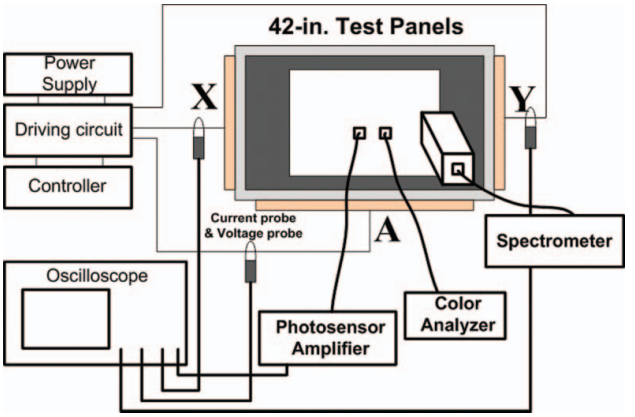

Figure 1. IR emission measurement system and 42-in HD test panel used in experiments.

and B cells. In addition, the effects of the phosphor layer thickness related to the discharge and radiation characteristics, such as luminance, visible light spectrum, and IR (Infrared) emission characteristics in a 42-in. HD plasma display panel.

Experimental Setup

Figure 1 shows the IR emission intensity measurement system and 42-in HD test panel used in the experiments. A photomultiplier tube (PMT), Spectrometer, and a waveform generator were used to measure the IR emission intensity, V_t closed-curves, the address discharge delay time, and the luminance efficiency in this study.

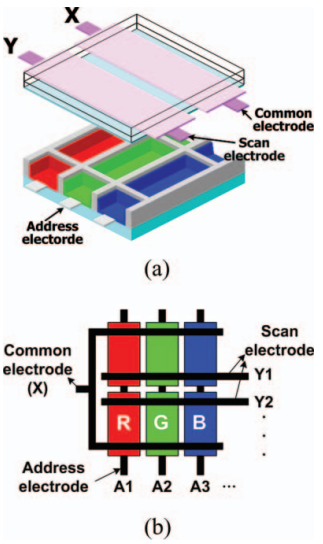

Figure 2. (a) Test panel structure and (b) schematic diagram of three electrodes in 42-in. HD PDP test panel employed in current study.

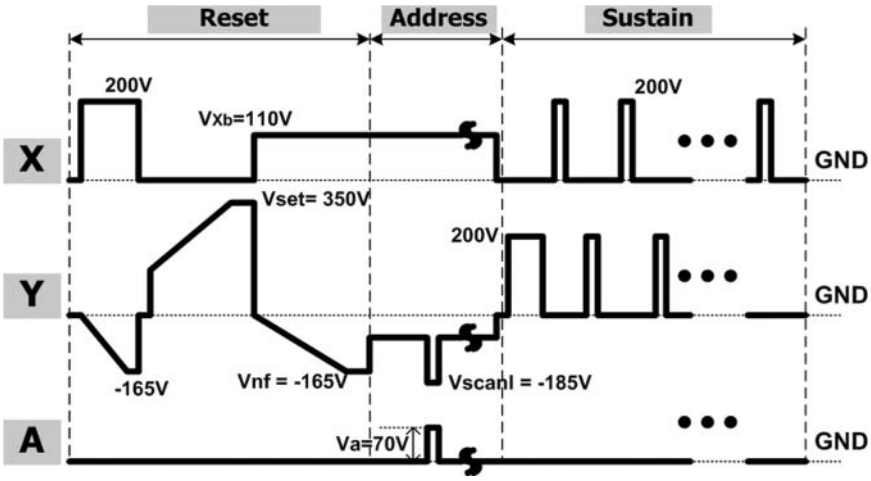

Figure 3. Schematic diagram of the driving waveform employed for measuring address discharge characteristics.

Figures 2(a) and (b) show the test panel structure and the schematic diagram of three electrodes in 42-in. HD plasma display test panel employed in the current study. As shown in Fig. 2(a), the test panel used in this work was a commercial 42-in. HD plasma display panel with a box-type barrier rib. The gas mixture and pressure of test panel were Ne-He-Xe(11%) and 420 Torr. The gap between the coplanar electrodes and the barrier rib height are fixed at 70 μm and 120 μm, respectively. As shown in Fig. 2(b), the scan (Y) and common (X) electrodes are common for the R, G, and B cells, implying that the same driving waveforms are applied to the X and Y electrodes except the address (A) electrode for the R, G, and B cells.

Figure 3 shows the schematic diagram of the driving waveform employed for measuring the address discharge characteristics with reset driving waveforms. In Fig. 3, the rising voltage Vset, is 350 V for reset period and the rising voltage. The negative falling voltage, Vnf is -165 V for reset period.

Result and Discussions

1. Comparison of Address Discharge Characteristics among commercial R, G, B Cells

Figure 4 shows the cell voltage of the measured Vt closed-curve among the R, G, and B cells without initial wall charges. In Fig. 4, VtXY means the discharge start threshold cell voltage between the X and Y electrodes, VtAY means the discharge start threshold cell voltage between the A and Y electrodes, VtAX means the discharge start threshold cell voltage between the A and X electrodes, VtYX means the discharge start threshold cell voltage between the Y and X electrodes, VtYA means the discharge start threshold cell voltage between the Y and A electrodes, and VtXA means the discharge start threshold cell voltage between the X and A electrodes. Table 1 shows the firing voltage of each discharge mode (X-Y, A-Y, A-X, Y-X, Y-A, X-A discharge) at the test panel. As shown in Fig. 4 and Table 1, the firing voltages for the X-Y, Y-X discharge (i.e., surface discharge and plate gap discharge under MgO cathode condition) were observed to be almost the same irrespective of the R, G, and B cells. For the Y-A, X-A discharge (i.e., plate gap discharge under a

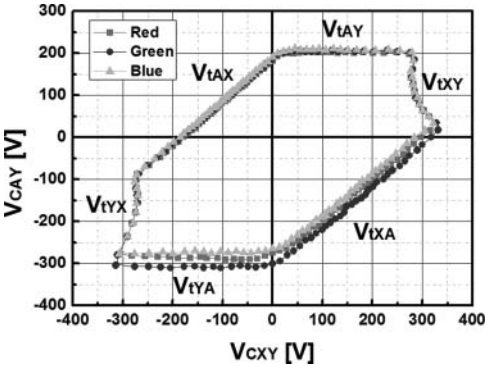

Figure 4. Cell voltage of measured Vt closed-curve among R, G, and B cells without initial wall charges.

phosphor cathode condition), the firing voltage of the G cell was observed to be higher than that of the R and B cells.

Figures 5(a) and (b) show the measured Vt closed-curves and the address discharge delay time after the reset discharge. As shown in Fig. 5(a), the Vt closed-curve of the G cell was shifted to the upward direction by about 3 V on the applied voltage plane. This means that the address discharge delay time of the G cell was slower than that of the other R and B cells. As a result, Fig. 5(b) show the address discharge characteristics after the reset-periods for the R, G, and B cells. As shown in Fig. 5(b), the address discharge delay time was observed to be slowest for the G cell.

2. Comparison of Discharge Characteristics by Various Thickness of Phosphor Layer

a. Luminance Efficiency Characteristics by Various Thickness of Phosphor Layer. Figure 6 and Table 2 show the SEM images and the thicknesses of bottom side of the red, green, and blue phosphor layers by control the wt% of phosphor powder in the paste. And the height of barrier rib is fixed by about 120 μm in this study. Case A, B, and C are 40, 45, and 50 wt% of phosphor powder in the paste, respectively.

Figure 7 shows the comparison of the luminance and visible light spectrum (400 nm $\sim$ 750 nm) under various thicknesses of the R, G, and B phosphor layer. As shown in Fig. 7, the luminance per net power is increased by about 11%, 9%, and 8% by increasing the

Table 1. Firing voltages of each discharge mode (X-Y, A-Y, A-X, Y-X, Y-A, X-A discharge) at the test panel

Firing voltage [V]		Red	Green	Blue
MgO Cathode	V_{tXY}	278	278	279
	V_{tAY}	202	205	208
	V_{tAX}	180	183	188
	V_{tYX}	271	270	272
Phosphor Cathode	V_{tYA}	268	307	273
	V_{tXA}	300	318	286

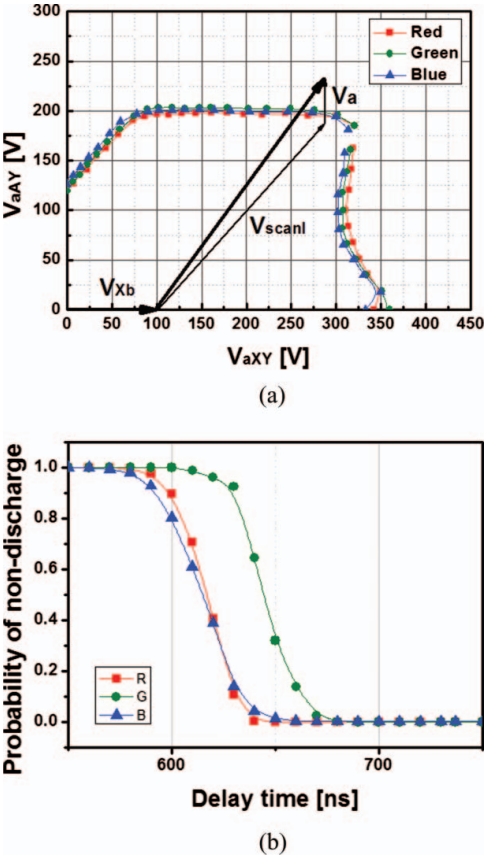

Figure 5. (a) Measured Vt closed-curves and (b) address discharge delay time after the reset discharge.

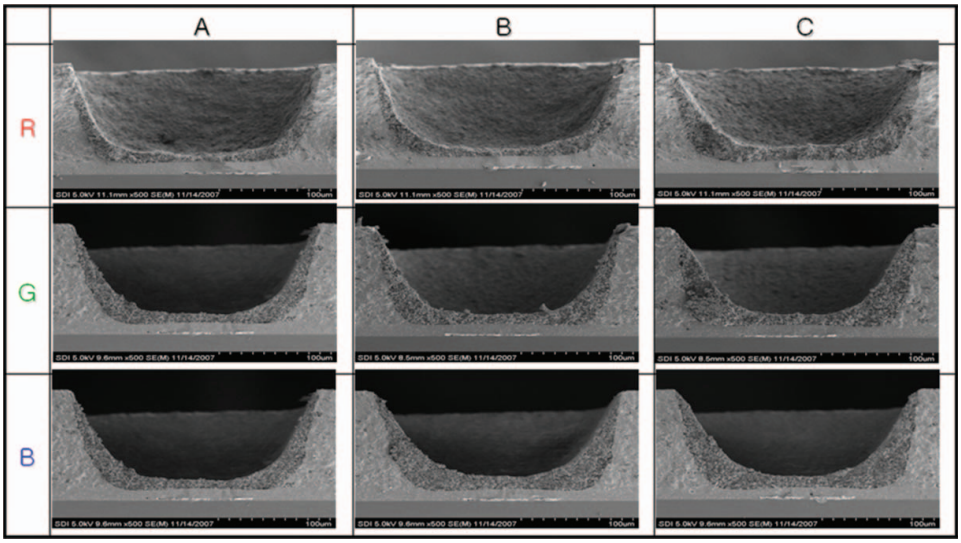

Figure 6. SEM images by thicknesses of red, green, and blue phosphor layers.

Table 2. Thicknesses of bottom side of the red, green, and blue phosphor layers

	Thickness of Phosphor layers [μm]		
	Red Panel	Green panel	Blue panel
A	7.53	7.53	9.52
B	8.33	10.31	12.69
C	16.26	11.50	15.70

Table 3. Firing voltages of each discharge mode by various thicknesses at the red phosphor

Firing voltage [V]		A	B	C
MgO Cathode	V_{tXY}	309	308	310
	V_{tAY}	213	215	219
	V_{tAX}	197	201	208
	V_{tYX}	298	299	301
Phosphor Cathode	V_{tYA}	322	335	344
	V_{tXA}	319	332	346

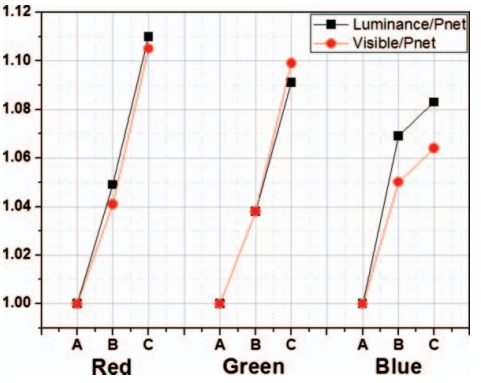

Figure 7. Comparison of luminance and visible light spectrum (400 nm $\sim$ 750 nm) under various thicknesses of R, G, and B phosphor layer.

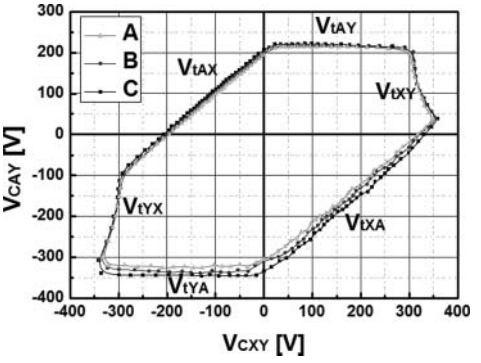

Figure 8. Measured Vt closed-curves for various phosphor thicknesses of Red phosphor without initial wall charges.

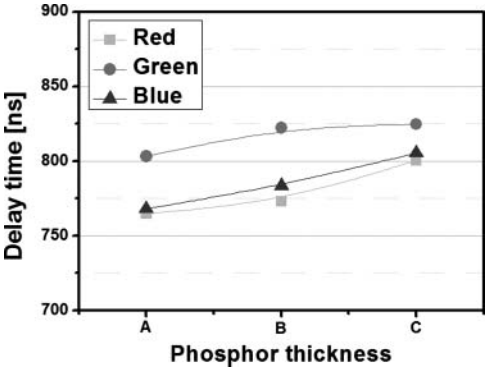

Figure 9. Changes in address discharge delay time relative to phosphor thicknesses.

thickness of the R, G, and B phosphor layer, respectively. And the visible light spectrum is also improved by about 10%, 10%, and 6% in case C. As a result, the luminous efficacy was observed to be improving by increase the phosphor layer thickness.

b. Address Discharge Delay Time Characteristics by Various Thickness of Phosphor Layer. Figure 8 shows the measured Vt closed-curves for the various phosphor thicknesses of the red phosphor without initial wall charges. As shown in Fig. 8, the firing voltage of the plate gap was increased by increasing the phosphor thickness. The A-Y firing voltage and Y-A firing voltage were increased by about 7 V and 20 $\sim$ 30 V, respectively even though the firing voltage of the surface gap was not increased. The detailed firing voltages are listed in Table 3.

Figure 9 shows the changes in the address discharge delay time relative to the phosphor thicknesses. The address discharge delay times were increased by increasing the phosphor thickness because the firing voltage of the plate gap was increased. As shown in Fig. 9, the address discharge delay time of the thinner G phosphor layer was almost the same as that of the thicker R and B phosphor layers. As a result, it is expected that the proper control of the phosphor thickness for R, G, and B cells will contribute to compensating the different address discharge delay phenomena irrespective of the R, G, and B cells.

Conclusions

The address discharge characteristics of ac-PDP strongly depend on the phosphor types. In addition, its address discharge characteristics also depend strongly on the phosphor thickness. Therefore, it is expected that the proper control of the phosphor thickness for R, G, and B cells will compensate the different address discharge delay phenomena irrespective of the phosphor types. In addition, the luminous efficacy was observed to be improving by increase the phosphor layer thickness.

Acknowledgment

This work was supported by Kyungpook National University Research Fund, 2012.

References

[1] Cho, B.-G., Lee, S. I., & Tae, H.-S. (2003). *IDW'03 Digest*, pp. 933–936.
[2] Park, H.-D., Kim, J.-H., Tae, H.-S., Kim, D. M., & Seo, J. H. (2011). *SID'11 Digest*, pp. 1468–1470.
[3] Park, H. D., Kim, J. Y., & Tae, H.-S. (2007). *SID'07 Digest*, pp. 569–572.
[4] Sakita, K., Takayama, K., Awamoto, K., & Hashimoto, Y. (2001). *SID'01 Digest*, pp. 1022–1025.
[5] Sakita, K., Takayama, K., Awamoto, K., & Hashimoto, Y. (2001). *Asia Display/IDW'01 Digest*, pp. 841–844.
[6] Park, H. D., Tae, H.-S., Jeong, H.-S., Hur, M., & Yoo, M. (2008). *IDW'08 Digest*, pp. 1921–1924.
[7] Chung, W. J., Shin, B. J., Kim, T. J., Bae, H. S., Seo, J. H., & Whang, K.-W. (2003). *IEEE Trans. Plasma Science*, *31*(5), 1038–1043.
[8] Tae, H.-S., Cho, K.-D., J., S.-H., & Choi, K.-C. (2001). *IEEE Trans. Electron Devices*, *48*(7), 1469–1472.
[9] Shin, B. J., Min, C.-S., & Seo, J.-H. (2011). *IEEE Trans. Plasma Science*, *39*(2), 695–699.